Article

Pyrazine-Containing Acene-Type Molecular Ribbons with up to 16 Rectilinearly Arranged Fused Aromatic Rings

Baoxiang Gao, Ming Wang, Yanxiang Cheng, Lixiang Wang, Xiabin Jing, and Fosong Wang

J. Am. Chem. Soc., **2008**, 130 (26), 8297-8306 • DOI: 10.1021/ja800311a • Publication Date (Web): 07 June 2008

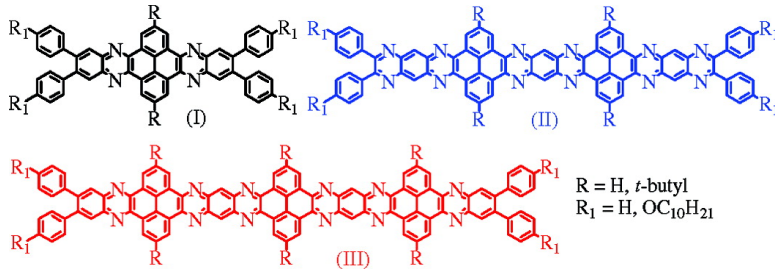

More About This Article

Additional resources and features associated with this article are available within the HTML version:

- Supporting Information
- Access to high resolution figures
- Links to articles and content related to this article
- Copyright permission to reproduce figures and/or text from this article

View the Full Text HTML

J|A|C|S
ARTICLES

Published on Web 06/07/2008

Pyrazine-Containing Acene-Type Molecular Ribbons with up to 16 Rectilinearly Arranged Fused Aromatic Rings

Baoxiang Gao,[†,‡] Ming Wang,[†] Yanxiang Cheng,[†] Lixiang Wang,[†,*] Xiabin Jing,[†] and Fosong Wang[†]

State Key Laboratory of Polymer Physics and Chemistry, Changchun Institute of Applied Chemistry, Chinese Academy of Sciences, Changchun 130022, P. R. China, and College of Chemistry and Environment Science, Hebei University, Baoding 071002, P. R. China

Received January 14, 2008; E-mail: lixiang@ciac.jl.cn

Abstract: A series of acene-type conjugated molecules (**1**−**5**) containing 2−6 pyrazine units and up to 16 rectilinearly arranged fused aromatic rings were synthesized by condensation coupling of 1,2-diamines and 1,2-diketones. The energy gap of the molecules estimated from absorption edge decreases with an increase in molecular length, indicating the well-delocalized nature of the molecules. The cyclic voltammetry measurements suggest that the *n*-type properties of these ribbonlike pyrazine derivatives are dependent on the molecular length and the number of the pyrazine units. As the number of pyrazine units and the molecular length increase, the first reduction wave onset is shifted from −1.16 to −0.62 V (vs Ag/AgCl), corresponding to the LUMO energy levels of −3.24 and −3.78 eV, respectively. These molecules tend to aggregate in solution more readily with an increase in molecular length, as evident by ^{1}H NMR and UV−vis absorption spectra. Introduction of *t*-butyl groups in pyrene units can noticeably suppress the aggregation of these molecules in solution. High electron affinity, high environmental stability, and ease of structural modification make these compounds excellent candidates as a new class of *n*-type semiconductors.

Introduction

Organic conjugated compounds are of current interest because of their potential applications in electronics and optoelectronics (e.g., organic light-emitting diodes, organic thin film transistors, and organic photovoltaic cells). *p*-Type and *n*-type organic materials, which are capable of transporting holes and electrons, respectively, are equally important in these applications. However, the vast majority of synthetic effort and structure−property studies in the field has been devoted to *p*-type organic molecules (electron donor or hole transport),[1–4] and only a limited number of *n*-type organic molecules have been synthesized, such as fluorinated aromatic compounds,[5–7] heteroaromatic compounds,[8,9] fullerene derivatives,[10] naphthalene, and perylene diimides.[11]

Heterocyclic aromatic compounds containing imine nitrogen atoms (═N─) generally have a less negative reduction potential compared to hydrocarbon analogues and heterocyclics containing oxygen or sulfur atoms.[8a] Computational investigations by Winkler and Houk showed that nitrogen-rich oligoacenes were promising candidates for *n*-type semiconductors.[12] In addition to strongly enhanced electron affinity, the successive replacement of CH moieties by nitrogen atoms in polycyclic aromatic hydrocarbons offers opportunities to manipulate the intermolecular interactions and molecular arrangements in the solid state and therefore to tune electronic properties.[12] For example, Brédas and co-workers predicted that the intermolecular bonding interaction was much more pronounced for hexaazatriphenylene dimer than that for triphenylene dimer.[13] Furthermore, one can also expect higher stability of ═N─ containing heteroacenes

[†] Chinese Academy of Sciences.
[‡] Hebei University.

(1) *Electronics Materials: The Oligomer Approach*; Müllen, K., Wegner, G., Eds.; Wiley VCH: Weinheim, Germany, 1998.
(2) Mitschke, U.; Bäuerle, P. *J. Mater. Chem.* **2000**, *10*, 1471–1507.
(3) Kraft, A.; Grimsdale, A. C.; Holmes, A. B. *Angew. Chem., Int. Ed.* **1998**, *37*, 402–428.
(4) Robinson, M. R.; Wang, S.; Bazan, G. C.; Cao, Y. *Adv. Mater.* **2000**, *12*, 1701–1704.
(5) (a) Fachetti, A.; Mushrush, M.; Katz, H. E.; Marks, T. J. *Adv. Mater.* **2003**, *15*, 33–38. (b) Sakamoto, Y.; Shingo, K.; Suzuki, T. *J. Am. Chem. Soc.* **2001**, *123*, 4643–4644. (c) Fachetti, A.; Deng, Y.; Wang, A.; Koide, Y.; Sirringhaus, H.; Marks, T. J.; Friend, R. H. *Angew. Chem., Int. Ed.* **2000**, *39*, 4547–4551. (d) Facchetti, A.; Yoon, M.-H.; Stern, C. L.; Hutchison, G. R.; Ratner, M. A.; Marks, T. J. *J. Am. Chem. Soc.* **2004**, *126*, 13480–13501.
(6) (a) Sakamoto, Y.; Suzuki, T.; Miura, A.; Fujikawa, H.; Tokito, S.; Taga, Y. *J. Am. Chem. Soc.* **2000**, *122*, 1832–1833. (b) Heidenhain, S. B.; Sakamoto, Y.; Suzuki, T.; Miura, A.; Fujikawa, H.; Mori, T.; Tokito, S.; Taga, Y. *J. Am. Chem. Soc.* **2000**, *122*, 10240–10241.
(7) Bao, Z.; Lovinger, A. J.; Brown, J. *J. Am. Chem. Soc.* **1998**, *120*, 207–208.
(8) (a) Tonzola, C. J.; Alam, M. M.; Kaminsky, W.; Jenekhe, S. A. *J. Am. Chem. Soc.* **2003**, *125*, 13548–13558. (b) Kwon, T. W.; Alam, M. M.; Jenekhe, S. A. *Chem. Mater.* **2004**, *16*, 4657–4666.
(9) Strukelj, M.; Papadimitrakopoulos, F.; Miller, T. M.; Rothberg, L. J. *Science* **1995**, *267*, 1969–1972.
(10) (a) Yang, Y.; Arias, F.; Echegoyen, L.; Chibante, F. L. P.; Flanagan, S.; Robertson, A.; Wilson, L. J. *J. Am. Chem. Soc.* **1995**, *117*, 7801–7804. (b) Boudon, C.; Gisselbrecht, J.-P.; Gross, M.; Herrmann, A.; Ruttimann, M.; Crassous, J.; Cardullo, F.; Echegoyen, L.; Diederich, F. *J. Am. Chem. Soc.* **1998**, *120*, 7860–7868. (c) Suzuki, T.; Maruyama, Y.; Akasaka, T.; Ando, W.; Kobayashi, K.; Nagase, S. *J. Am. Chem. Soc.* **1994**, *116*, 1359–1363. (d) Hummelen, J. C.; Knight, B. W.; LePeq, F.; Wudl, F.; Yao, J.; Wilkins, C. L. *J. Org. Chem.* **1995**, *60*, 532–538. (e) Da Ros, T.; Prato, M.; Carano, M.; Ceroni, P.; Paolucci, F.; Roffia, S. *J. Am. Chem. Soc.* **1998**, *120*, 11645–11648. (f) Thompson, B. C.; Fréchet, J. M. J. *Angew. Chem., Int. Ed.* **2008**, *47*, 58–77.

than hydrocarbon analogues toward photooxidation or Diels−Alder dimerization (two major degradation pathways in acenes[14]).

As a typical nitrogen-containing heterocyclic compound, pyrazine has been proven as a valuable building block for thermally stable polymers and electron-accepting π-conjugated polymers.[15] Early studies on thermally stable pyrazine-containing polymers were reviewed by Yu et al.[15c] Recently, pyrazine is frequently used in the design and synthesis of *n*-type organic semiconductors, such as pyrazinoquinoxaline derivatives,[16] hexaazatriphenylenes,[17] diquinoxalino[2,3-*a*:2′,3′-*c*] phenazines,[18] and quinoxalino[2′,3′,9,10] phenanthro[4,5-*abc*] phenazines,[19] owing to its electron-deficient characteristic. The electron affinity of the resultant compounds is noticeably higher than that of analogous polycyclic aromatic hydrocarbons and can be adjusted by altering molecular structures or substitution patterns. In particular, some of these compounds exhibit high charge carrier mobility[16a,18a–c] and intriguing self-assembling properties.[17c–g,18d–h,19] It is well known that many properties of conjugated molecules are molecular size-dependent.[20] Thus, one can expect that one-dimensional multipyrazine-containing acene-type conjugated molecules exhibit some intriguing *n*-type semiconducting and self-assembling properties that depend on the molecular length and the number of pyrazine units. We herein report the synthesis and characterization of a series of pyrazine-containing acene-type conjugated molecules with up to six pyrazine units and 16 rectilinearly arranged fused aromatic rings and some unique structure−property relationships of this class of conjugated molecules.

Results and Discussion

All pyrazine-containing acene-type molecules (PAMs) prepared in this work are depicted in Chart 1. According to the distribution of pyrazine units, these compounds can be divided into three classes: (I) compound **1**, in which two pyrazine units are separated by a pyrene unit; (II) compounds **2** and **4**, in which two pyrazinoquinoxaline units are separated by a pyrene unit; and (III) compounds **3** and **5**, which have both structural features of types I and II. Four terminal phenyl groups with alkoxy chains were introduced to improve the solubility of the intermediates and the final products. Introduction of *t*-butyl substituents in pyrene units was proposed to further improve the solubility and depress the aggregation of the compounds for ease of purification and characterization.

The synthesis of compounds **1**−**5** is outlined in Schemes 1 and 2. Suzuki coupling reactions between 4,5-dibromo-1,2-phenylenediamine (**6**)[21] and phenyl boronic acids **7a** and 7**b** gave diamines **8a** (83%) and **8b** (78%), respectively. Following a typical condensation-coupling reaction between 1,2-diamines and 1,2-diketones,[15a] a twofold condensation between **8** and pyrene-4,5,9,10-teteranes **9a** and **9b**[22] in refluxing acetic acid afforded compounds **1a**−**c** in high yields (75−92%).

The synthesis of monocondensation intermediates **10a** and **10b** is a key step to longer PAMs **3** and **5**. The monocondensation was successful by dropwise addition of **8b** to an excess of **9** in acetic acid at 50 °C, yielding **10a** (58%) and **10b** (52%) as precipitates from the reaction medium. An attempt to further condense compounds **10** and **11** in refluxing acetic acid was not successful in yielding **3**. By using high boiling point *m*-cresol, which is often used in the synthesis of high molecular weight polyquinoxalines,[15b] compounds **3a** and **3b** were obtained in yields of 46 and 51%, respectively. However, condensation of **10a** and 6,7,15,16-teteraminoquinoxalino[2,3,9,10]phenanthro[4,5-*abc*]phenazine[23] in *m*-cresol did not produce the target compound because of extremely low solubility of the monocondensation intermediate. Then one pair of *t*-butyl groups in each pyrene unit was introduced to improve the solubility, and as a result compound **5** was successfully prepared in 46% yield. To synthesize compounds **2** and **4**, 4,4′-didecyloxybenzil (**13**)[24] was first condensed with 1,2-dinitro-4,5-diaminobenzene (**14**)

(11) (a) Katz, H. E.; Lovinger, A. J.; Johnson, J.; Kloc, C.; Siegrist, T.; Li, W.; Lin, Y.-Y.; Dodabalapur, A. *Nature* **2000**, *404*, 478–481. (b) Gregg, B. A.; Cormier, R. A. *J. Am. Chem. Soc.* **2001**, *123*, 7959–7960. (c) Jones, B. A.; Facchetti, A.; Wasielewski, M. R.; Marks, T. J. *J. Am. Chem. Soc.* **2007**, *129*, 15259–15278.
(12) Winkler, M.; Houk, K. N. *J. Am. Chem. Soc.* **2007**, *129*, 1805–1815.
(13) Cornil, J.; Lemaur, V.; Calbert, J. P.; Brédas, J. L. *Adv. Mater.* **2002**, *14*, 726–729.
(14) (a) Payne, M. M.; Odom, S. A.; Parkin, S. R.; Anthony, J. E. *Org. Lett.* **2004**, *6*, 3325–3328. (b) Maliakal, A.; Raghavachari, K.; Katz, H.; Chandross, E.; Siegrist, T. *Chem. Mater.* **2004**, *16*, 4980–4986. (c) Payne, M. M.; Parkin, S. R.; Anthony, J. E.; Kuo, C.; Jackson, T. N. *J. Am. Chem. Soc.* **2005**, *127*, 8028–8029. (d) Chien, S.-H.; Cheng, M.-F.; Lau, K. C.; Li, W. K. *J. Phys. Chem. A* **2005**, *109*, 7509–7518.
(15) (a) Stille, J. K.; Mainen, E. L. *Macromolecules* **1968**, *1*, 36–42. (b) Imai, K.; Kurihara, M.; Mathias, L.; Wittmann, J.; Alston, W. B.; Stille, J. K. *Macromolecules* **1973**, *6*, 158–162. (c) Yu, L.; Chen, M.; Dalton, L. R. *Chem. Mater.* **1990**, *2*, 649–659. (d) Yamamoto, T.; Sugiyama, K.; Kushida, T.; Inoue, T.; Kanbara, T. *J. Am. Chem. Soc.* **1996**, *118*, 3930–3937. (e) Zhang, C. Y.; Tour, J. M. *J. Am. Chem. Soc.* **1999**, *121*, 8783–8790. (f) Jenekhe, S. A. *Macromolecules* **1991**, *24*, 1–10.
(16) (a) Nishida, J.-i.; Naraso; Murai, S.; Fujiwara, E.; Tada, H.; Tomura, M.; Yamashita, Y. *Org. Lett.* **2004**, *6*, 2007–2010. (b) Miao, S.; Smith, M. D.; Bunz, U. H. F. *Org. Lett.* **2006**, *8*, 757–760.
(17) (a) Beeson, J. C.; Fitzgerald, L. J.; Gallucci, J. C.; Gerkin, R. E.; Rademacher, J. T.; Czarnik, A. W. *J. Am. Chem. Soc.* **1994**, *116*, 4621–4622. (b) Secondo, P.; Fages, F. *Org. Lett.* **2006**, *8*, 1311–1314. (c) Gearba, R. I.; Lehmann, M.; Levin, J.; Ivanov, D. A.; Koch, M. H. J.; Barberá, J.; Debije, M. G.; Piris, J.; Geerts, Y. H. *Adv. Mater.* **2003**, *15*, 1614–1618. (d) Ishi-i, T.; Hirayama, T.; Murakami, K.-i.; Tashiro, H.; Thiemann, T.; Kubo, K.; Mori, A.; Yamasaki, S.; Akao, T.; Tsuboyama, A.; Mukaide, T.; Ueno, K.; Mataka, S. *Langmuir* **2005**, *21*, 1261–1268. (e) Chang, T.-H.; Wu, R.-R.; Chiang, M. Y.; Liao, S.-C.; Ong, C. W.; Hsu, H.-F.; Lin, S.-Y. *Org. Lett.* **2005**, *7*, 4075–4078. (f) Ishi-i, T.; Murakami, K.; Imai, Y.; Mataka, S. *Org. Lett.* **2005**, *7*, 3175–3178. (g) Ishi-i, T.; Yaguma, K.; Kuwahara, R.; Taguri, Y.; Mataka, S. *Org. Lett.* **2006**, *8*, 585–588.
(18) (a) Lemaur, V.; da Silva Filho, D. A.; Coropceanu, V.; Lehmann, M.; Geerts, Y.; Piris, J.; Debije, M. G.; van de Craats, A. M.; Senthilkumar, K.; Siebbeles, L. D. A.; Warman, J. M.; Brédas, J.-L.; Cornil, G. *J. Am. Chem. Soc.* **2004**, *126*, 3271–3279. (b) Kaafarani, B. R.; Kondo, T.; Yu, J.; Zhang, Q.; Dattilo, D.; Risko, C.; Jones, S. C.; Barlow, F.; Domercq, B.; Amy, F.; Kahn, A.; Brédas, J.-L.; Kippelen, B.; Marder, S. R. *J. Am. Chem. Soc.* **2005**, *127*, 16358–16359. (c) Lehmann, M.; Kestemont, G.; Aspe, R. G.; Buess-Herman, C.; Koch, M. H. J.; Debije, M. G.; Piris, J.; de Haas, M. P.; Warman, J. M.; Watson, M. D.; Lemaur, V.; Cornil, J.; Geerts, Y. H.; Gearba, R. I.; Ivanov, D. A. *Chem.−Eur. J.* **2005**, *11*, 3349–3362. (d) Yip, H.-L.; Zou, J.; Ma, H.; Tuan, Y.; Tucker, N. M.; Jen, A. K.-Y. *J. Am. Chem. Soc.* **2006**, *128*, 13042–13043. (e) Ong, C. W.; Liao, S.-C.; Chang, T.-H.; Hsu, H.-F. *J. Org. Chem.* **2004**, *69*, 3181–3185. (f) Ong, C. W.; Liao, S.-C.; Chang, T.-H.; Hsu, H.-F. *Tetrahedron Lett.* **2003**, *44*, 1477–1480. (g) Kestemont, G.; de Halleux, V.; Lehmann, M.; Ivanov, D. A.; Watson, M.; Geerts, Y. H. *Chem. Commun.* **2001**, 2074–2075. (h) Bock, H.; Babeau, A.; Seguy, I.; Jolinat, P.; Destruel, P. *ChemPhysChem* **2002**, *3*, 532–535.
(19) (a) Hu, J.; Zhang, D.; Jin, S.; Cheng, S. Z. D.; Harris, F. W. *Chem. Mater.* **2004**, *16*, 4912–4915. (b) Kaafarni, B. R.; Lucas, L. A.; Wex, B.; Jabbour, G. E. *Tetrahedron Lett.* **2007**, *48*, 5995–5998.
(20) Gierschner, J.; Cornil, J.; Egelhaaf, H.-J. *Adv. Mater.* **2007**, *19*, 173–191.
(21) Cheeseman, G. W. H. *J. Chem. Soc.* **1962**, *84*, 1170–1176.
(22) Hu, J.; Zhang, D.; Harris, F. W. *J. Org. Chem.* **2005**, *70*, 707–708.
(23) Arnold, F. E. *J. Polym. Sci., Part A: Polym. Chem.* **1970**, *8*, 2079–2089.
(24) Hiroko, H.; Akira, T.; Hiroshi, H.; Takumi, O.; Kazuchika, O. *J. Mater. Chem.* **2001**, *11*, 1063–1071.

Chart 1. Chemical Structures of Compounds **1**−**5**

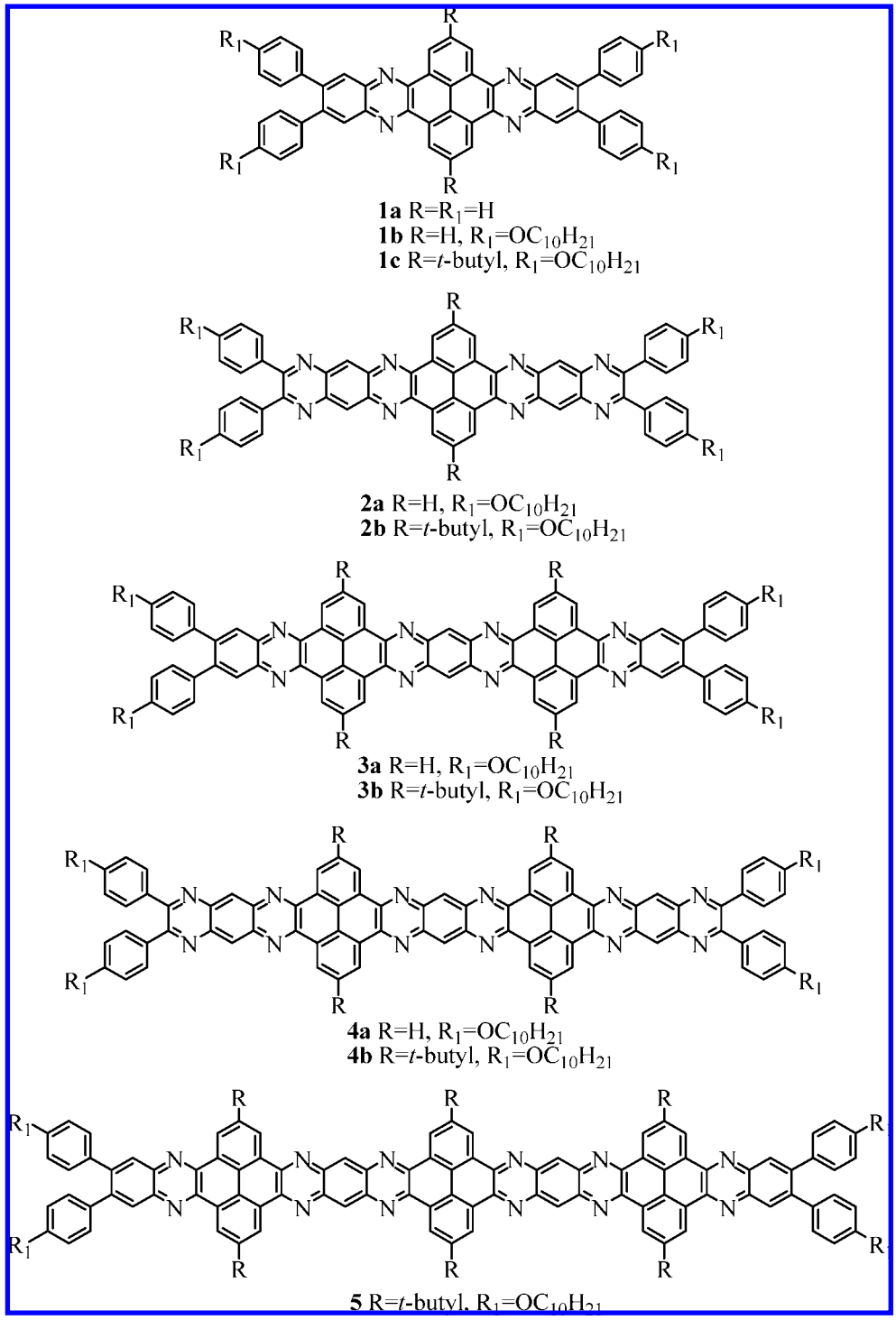

to give **15**, which was reduced with hydrazine in the presence of Pd/C to afford diamine **16** in a yield of 80%. The diamines quickly changed from yellow to pink and then brown if exposed to air. Therefore, the freshly prepared diamine **16** was subsequently condensed with pyrene-4,5,9,10-teteranes in refluxing acetic acid to give compounds **2a** and **2b**. The intermediates **17a** and **17b** were obtained by dropwise addition of the 1,2-diamine **16** to an excess of pyrene-4,5,9,10-teteranes **9a** and **9b** at 50 °C, respectively, in the same way as for the preparation of **10**. Then the twofold condensation reactions of **17** with the teteramine **11** in *m*-cresol gave the PAMs **4a** and **4b** in yields of 40 and 42%, respectively. Very low solubility of **4a** in common organic solvents makes it practically impossible for chromatographic purification. In comparison, the solubility of **4b** is high enough for purification by column chromatography. Unlike hydrocarbon acenes,[25] PAMs **1**−**5** show very good environmental stability, as evidenced by the unchanged absorption

(25) (a) Fang, T. Heptacene, Octacene, Nonacene, Supercene and Related Polymers. Ph.D. Thesis, University of California, Los Angeles, CA, 1986. (b) Bendikov, M.; Wudl, F.; Perepichka, D. F. *Chem. Rev.* **2004**, *104*, 4891–4946.

Scheme 1. Synthesis of Compounds **1**, **3**, and **5**[a]

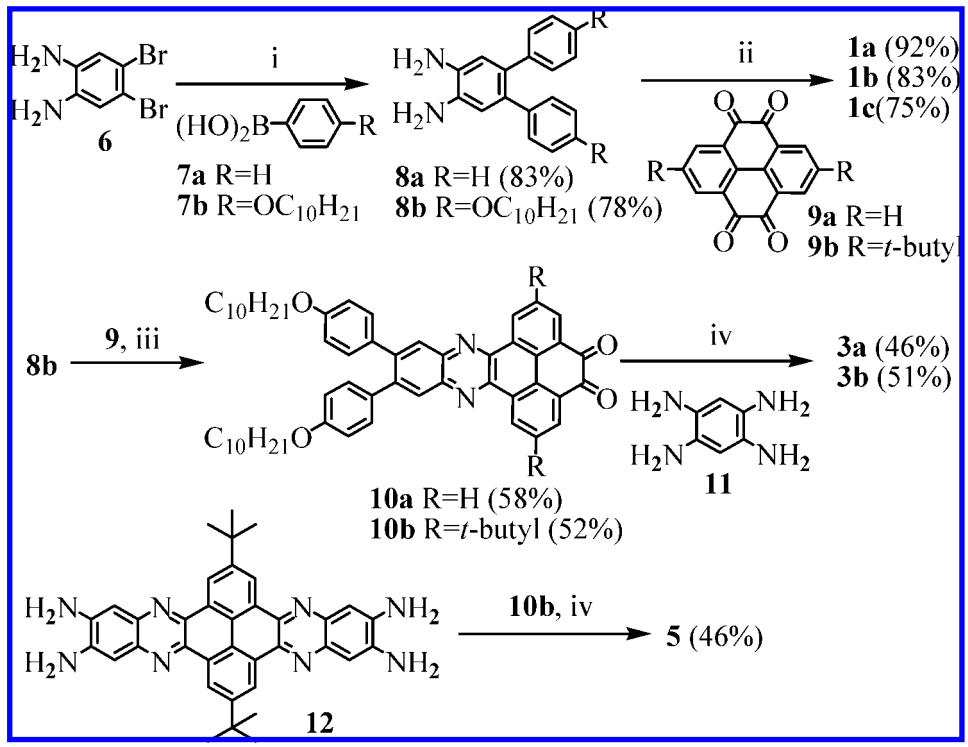

[a] (i) $Pd(PPh_3)_4$, toluene, K_2CO_3 (aq), 85 °C; (ii) AcOH, reflux; (iii) AcOH, 50 °C; (iv) *m*-cresol, 180 °C.

Scheme 2. Synthesis of Compounds **2** and **4**[a]

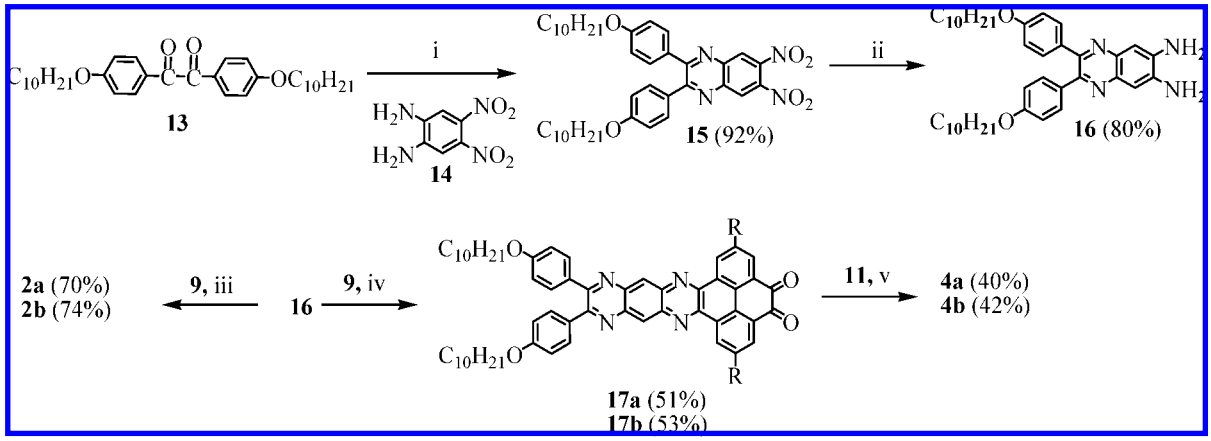

[a] (i) AcOH, 80°C; (ii) Pd/C, $NH_2NH_2 \cdot H_2O$, EtOH, reflux; (iii) AcOH, reflux; (iv) AcOH, 50°C; (v) *m*-cresol, 180 °C.

spectra of the samples in solution left in air and under the laboratory lighting for up to one month. Furthermore, PAMs are thermally stable in nitrogen without any weight loss up to 400 °C as revealed by thermogravimetric analysis. Chemical structures of all the PAMs were confirmed by spectroscopic means and elemental analysis (Supporting Information).

Single crystals of **1a** suitable to X-ray crystallographic analysis were successfully obtained by slow evaporation of its dichloromethane solution at room temperature. As shown in Figure 1, the central fused aromatic segment deviates from planar geometry. The molecules adopt a 1-D face-to-face $\pi-\pi$ stacking with a distance of 3.48 Å. The neighboring molecules are slipped with respect to each other along the molecular long axis by 4.77 Å. The electron-deficient pyrazine rings are overlapped with the electron-rich pyrene rings. This packing motif suggests the presence of strong intermolecular interaction, ideal for easy intermolecular charge carrier transport.[26]

The absorption and photoluminescence (PL) spectra of compounds **1**−**5** were recorded in chloroform (2×10^{-6} mol/L), and the data are listed in Table 1. The introduction of four phenyl groups in **1a** resulted in a red-shift of 24 nm in absorption, while comparing **1a** with the previously reported unsubstituted analogues.[15a] It was found that the photophysical properties of PAMs were almost independent of solubi-

(26) (a) Naraso; Nishida, J.-i.; Ando, S.; Yamaguchi, J.; Itaka, K.; Koinuma, H.; Tada, H.; Tokito, S.; Yamashita, Y. *J. Am. Chem. Soc.* **2005**, *127*, 10142–10143. (b) Brédas, J. L.; Calbert, J. P.; Da Silva Filho, D. A.; Cornil, J. *Proc. Natl. Acad. Sci. U.S.A.* **2002**, *99*, 5804–5809. (c) Li, X.-C.; Sirringhaus, H.; Garnier, F.; Holmes, A. B.; Moratti, S. C.; Feeder, N.; Clegg, W.; Teat, S. J.; Friend, R. H. *J. Am. Chem. Soc.* **1998**, *120*, 2206–2207.

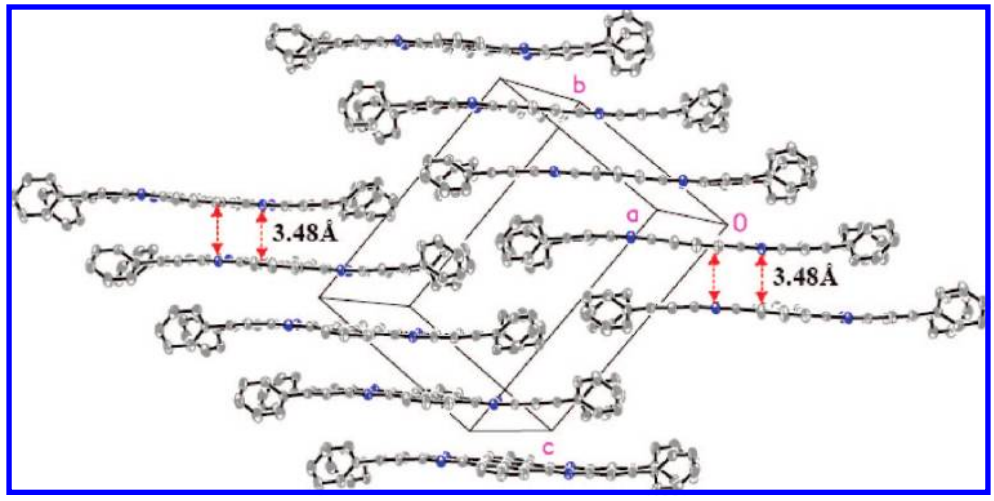

Figure 1. Crystal packing of compound **1a**.

Table 1. UV−Vis Absorption Maxima (λ_{abs}), Photoluminescence Maxima (λ_{em}), Photoluminescence Quantum Yields (Φ), Energy Gaps (E_{gap}), First Reduction Potentials ($E^{red}_{1/2}$) and Onsets (E^{red}_{onset}), and LUMO Energy Levels of Compounds **1**−**5**

compd	λ_{abs} ($\varepsilon/10^{-5}$ [mol/L·cm])[a] λ_{abs}^{0-1} (nm)	λ_{abs}^{0-0} (nm)	λ_{em} (nm)	Φ[b] (%)	E_{gap}[c] (eV)	$E^{red}_{1/2}$[d] $E_{1/2}^{1}$ (V)	$E_{1/2}^{2}$ (V)	$E_{1/2}^{3}$ (V)	E^{red}_{onset}[e] (V)	LUMO[f] (eV)[e]
1a	408 (0.59)	433 (0.96)	452	73	2.78	−1.20	−1.38		−1.15	−3.25
1b	418 (0.86)	443 (0.53)	490	86	2.66	−1.20	−1.37		−1.13	−3.27
1c	418 (0.59)	443 (0.88)	480	91	2.65	−1.22	−1.40		−1.16	−3.24
2a	471 (0.97)	500 (1.57)	553	65	2.36	−0.80	−1.43		−0.71	−3.69
2b	471 (1.04)	500 (1.64)	533	82	2.34	−0.78	−1.37		−0.70	−3.70
3a	500 (0.48)	538 (0.25)	658	6	2.22	−0.80	−1.37		−0.69	−3.71
3b	494 (0.50)	525 (0.59)	652	4	2.25	−0.78	−1.38		−0.67	−3.73
4a	500 (0.79)	531 (0.40)			2.25					
4b	500 (1.36)	529 (0.83)			2.22	−0.73	−1.23	−1.47	−0.64	−3.76
5	508 (0.47)	538 (0.34)			2.18	−0.71	−1.22	−1.42	−0.62	−3.78

[a] Measured in chloroform with a concentration of 2.0×10^{-6} mol/L. [b] Measured in chloroform with Nile red in 1,4-dioxane (Φ = 68%) as a reference. [c] Estimated from absorption onset. [d] Obtained from differential pulse voltammetry experiments. [e] Calculated from cyclic voltammograms. [f] Estimated from E^{red}_{onset}.

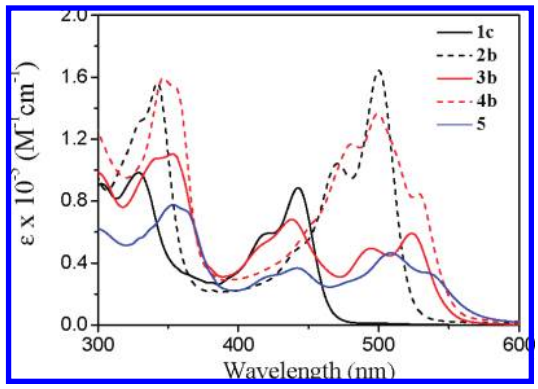

Figure 2. UV−vis absorption spectra of compounds **1c**, **2b, 3b**, **4b**, and **5** in chloroform with a concentration of 2×10^{-6} mol/L.

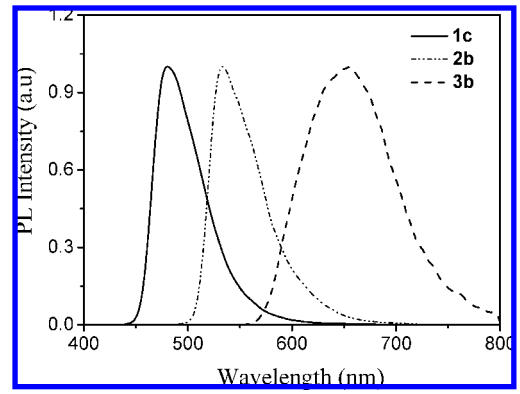

Figure 3. Photoluminescence spectra of compounds **1c**, **2b**, and **3b** in chloroform with a concentration of 2×10^{-6} mol/L.

lizing substituents, and the absorptions were red-shifted with increase of the molecular length. Displayed in Figure 2 are the absorption spectra of **1c**, **2b**, **3b**, **4b**, and **5**. All spectra are well-resolved with clear vibronic structures, which is consistent with the rigid structural feature of the compounds. Compound **1c** exhibits an absorption band at 443 nm, corresponding to the 0−0 transition. The 0−0 absorption is red-shifted to 500, 525, 529, and 538 nm for **2b**, **3b**, **4b**, and **5**, respectively, indicative of the lowered energy gap and the increased conjugation length with increase of the molecular length. However, it should be pointed out that the energy gaps of compounds **1**−**5** are saturated rapidly as the molecular length increases, in contrast to those of previously reported hydrocarbon acenes.[14c] One of the reasons may be the cross-conjugation in compounds **1**−**5** due to the incorporation of pyrene units in the molecular backbone. The normalized PL spectra of compounds **1c**, **2b**, and **3b** are presented in Figure 3. Relative to the molecular length, the emission maximum is red-shifted from 480 nm for **1c** to 533 nm for **2b**, and then to 652 nm for **3b**. Meanwhile, the PL quantum yields (Φ_{PL}) dramatically decrease from 91 and 82% for **1c** and **2b**, respectively, to 4% for **3b**. Particularly, PL was not

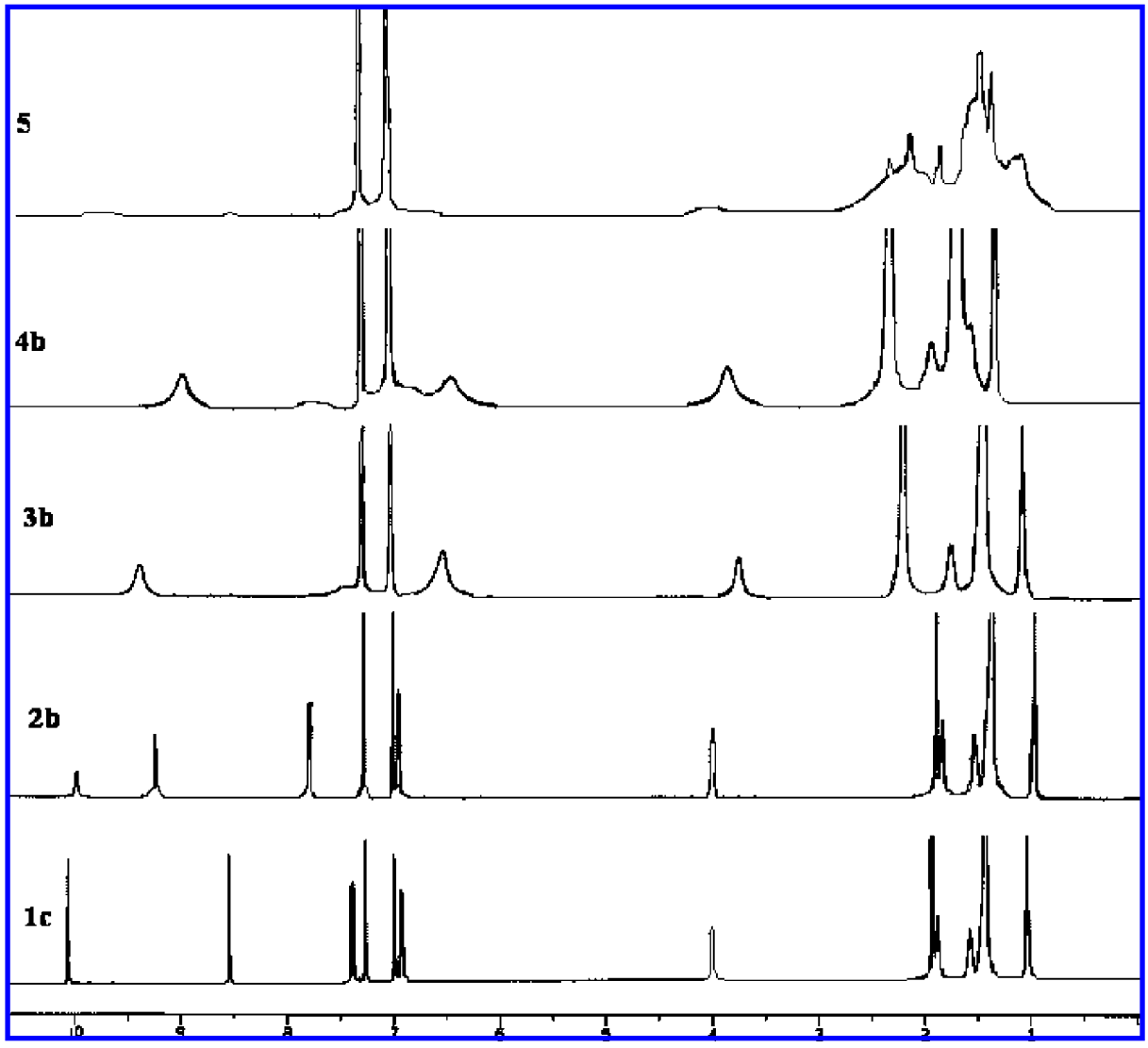

Figure 4. ^{1}H NMR spectra of **1c**, **2b**, **3b**, **4b**, and **5** in 1,2-dichlorobenzene-d_4 at 120 °C.

detectable for the longer molecular ribbons **4b** and **5**. The corresponding compounds without *t*-butyl substituents follow the same trend for their PL properties, as shown in Table 1. One of the main reasons for low Φ_{PL} should be attributed to the increased π-aggregation tendency for long, flat molecules. It was reported by Müllen et al. that strong aggregation led to a complete quenching of fluorescence for large discotic polycyclic aromatic hydrocarbons.[27]

The aggregation tendency of PAMs in dilute solution was studied by means of ^{1}H NMR and UV−vis spectroscopic methods. Figure 4 shows the ^{1}H NMR spectra of **1c**, **2**−**4b**, and **5** in 1,2-dichlorobenzene-d_4 at 120 °C. For compounds **1c** and **2b**, the spectra are well-resolved. With an increase in molecular length, the spectra are characterized by significant line broadening together with upfield shift. Particularly, only resonances from the alkoxy side chains and *t*-butyl groups can be well observed for compound **5**. The NMR studies indicate the correlation between the aggregation or $\pi-\pi$ interaction tendency and the molecular length, identical to the phenomena observed in other polycyclic aromatic systems.[28] In general, the $\pi-\pi$ interactions of aromatic molecules can lead to additional ring-current effects. As a result, the ^{1}H NMR spectra of strongly aggregated molecules are different from those of isolated monomeric species and are sensitive to solution concentration and temperature.[29] Shown in Figure 5 are concentration-dependent ^{1}H NMR spectra of compounds **1b**, **2a**, **1c**, and **2b** in *d*-chloroform. As the concentration increases from 3×10^{-4} to 6×10^{-3} mol/L, the chemical shifts of aromatic protons H-a, H-b, H-c, H-d, and H-e in compound **1b** are shifted upfield by 0.28, 0.41, 0.14, 0.10, and 0.05 ppm, respectively. The chemical shift of the aromatic proton H-b is most sensitive to the concentration, suggesting that the proton H-b is the closest to the centroid of the neighboring molecules in π-aggregation. The ^{1}H NMR spectra of compound **2a** are featured by upfield

(27) Wasserfallen, D.; Kastler, M.; Pisula, W.; Hofer, W. A.; Fogel, Y.; Wang, Z.; Müllen, K. *J. Am. Chem. Soc.* **2006**, *128*, 1334–1339.

(28) (a) Tomovic, Z.; Watson, M. D.; Müllen, K. *Angew. Chem., Int. Ed.* **2004**, *43*, 755–758. (b) Zhi, L.; Wu, J.; Müllen, K. *Org. Lett.* **2005**, *7*, 5761–5764. (c) Wu, J.; Watson, M. D.; Müllen, K. *Angew. Chem., Int. Ed.* **2003**, *42*, 5329–5333.

(29) (a) Hunter, C. A.; Sanders, J. K. M. *J. Am. Chem. Soc.* **1990**, *112*, 5525–5534. (b) Wu, J.; Fechtenkotter, A.; Gauss, J.; Watson, M. D.; Kastler, M.; Fechtenkotter, C.; Wagner, M.; Mullen, K. *J. Am. Chem. Soc.* **2004**, *126*, 11311–11321.

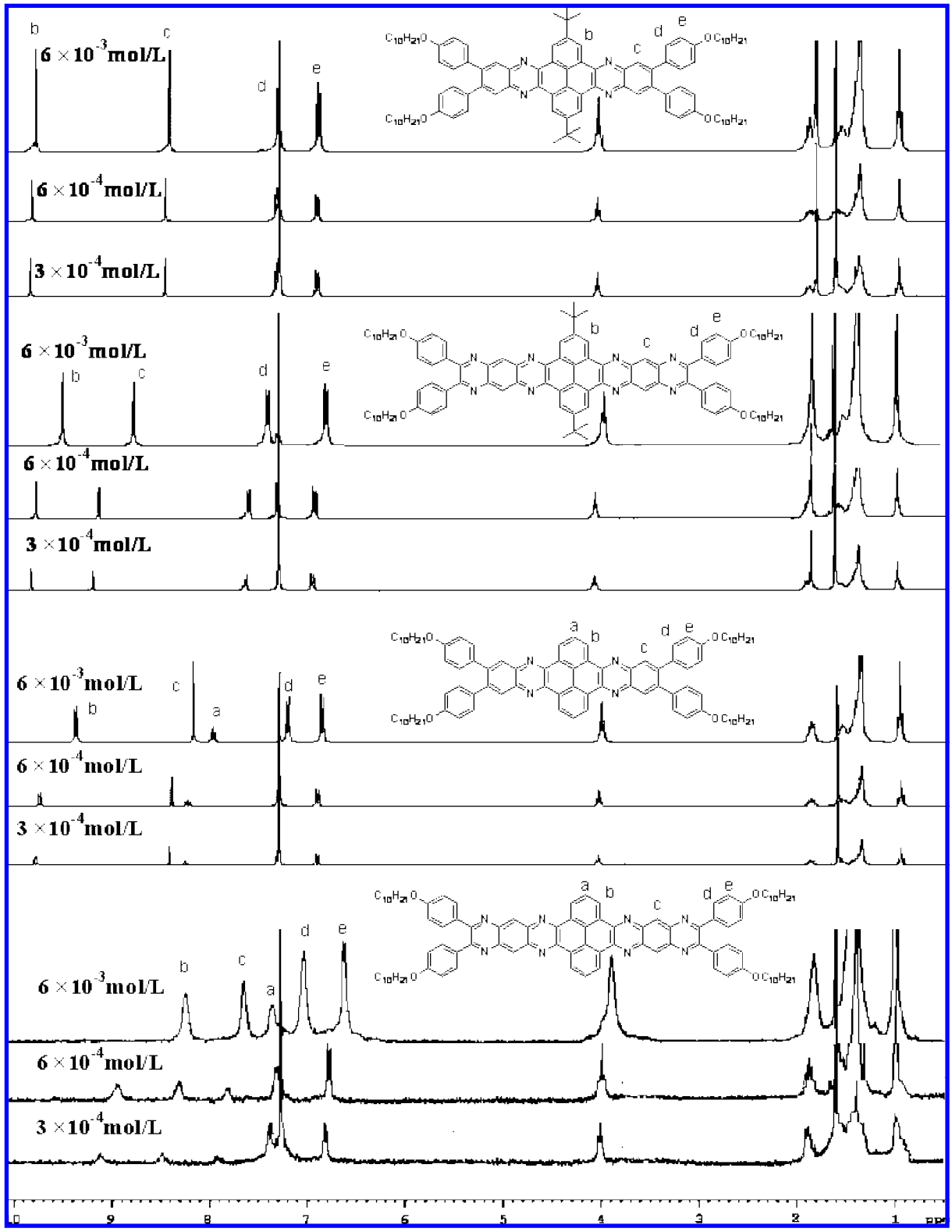

Figure 5. Concentration-dependent ^{1}H NMR spectra of **1b**, **2a**, **1c**, and **2b** in $CDCl_3$ at 20 °C.

shift of 0.88 ppm from 3×10^{-4} to 6×10^{-3} mol/L, and broad line shape even at 3×10^{-4} mol/L, indicating a dramatically increased aggregation tendency. Introduction of *t*-butyl groups in pyrene unit can noticeably suppress the aggregation of the compounds. The resonances of H-b in compounds **1c** and **2b** only shift to the upfield by 0.05 and 0.31 ppm, respectively.

Displayed in Figure 6 are temperature-dependent ^{1}H NMR spectra of compounds **1b**, **2a**, **1c**, and **2b** at a concentration of 6.0×10^{-3} mol/L in 1,1,2,2-tetrachloroethane-d_2. Similar to the concentration dependence, compound **2a** exhibits the strongest aggregation tendency. At 20 °C, the ^{1}H NMR spectrum of compound **2a** is featured by very weak and broad signals. By increasing the temperature, the signals become sharp and

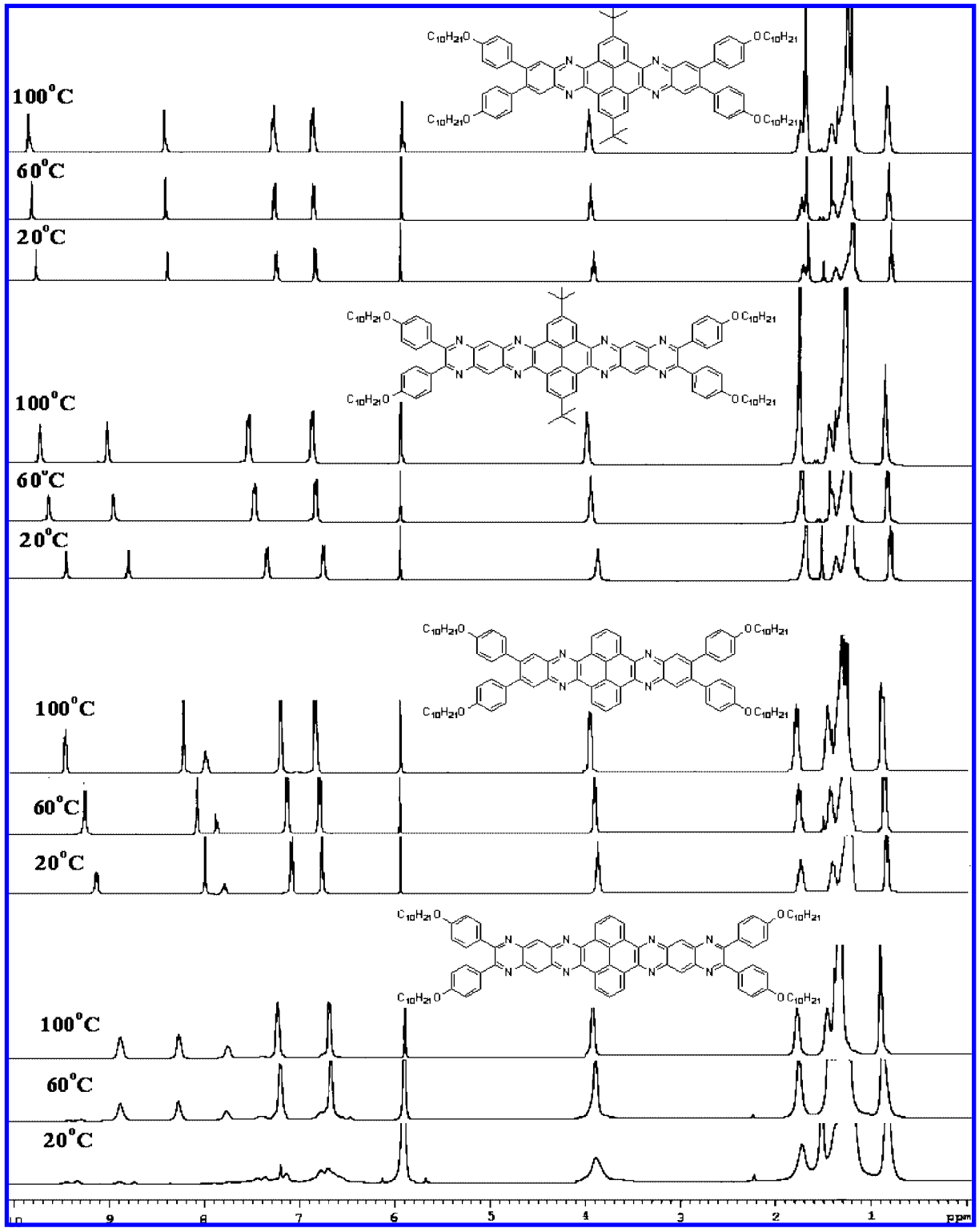

Figure 6. Temperature-dependent ^{1}H NMR spectra of **1b**, **2a**, **1c**, and **2b** in 1,1,2,2-tetrachloroethane-d_2 with a concentration of 6×10^{-3} mol/L.

distinct. However, the spectrum at 100 °C is still more poorly resolved in comparison with that of other three compounds.

To give a quantitative depiction of the aggregation tendency of PAMs, the association constants of **1b**, **1c**, **2a**, and **2b** in *d*-chloroform at 20 °C (Table 2) were determined by analyzing ^{1}H NMR chemical shifts of H-b at the different concentrations with the equal K (EK) model of indefinite self-association.[30] Compounds **1b** and **2a** exhibit a K_E value of 614 ± 61 and 6818 ± 682 M^{-1}, respectively. These values are much higher than those of phenylacetylene macro-

(30) (a) Zhang, J.; Moore, J. S. *J. Am. Chem. Soc.* **1992**, *114*, 9701–9702. (b) Shetty, A. S.; Zhang, J.; Moore, J. S. *J. Am. Chem. Soc.* **1996**, *118*, 1019–1027. (c) Martin, R. B. *Chem. Rev.* **1996**, *96*, 3043–3064. (d) Horman, I.; Dreux, B. *Helv. Chim. Acta* **1984**, *67*, 754–764.

Table 2. Association Constants of Compounds **1b**, **2a**, **1c**, and **2b** in $CDCl_3$ at Room Temperature As Calculated from Chemical Shift of the Aromatic Proton H-b

compound	1b	2a	1c	2b
K_E (L/mol)	614 ± 61	6818 ± 620	18± 2	326 ± 33

cycles[30a,b,31] and perylene tetracarboxylic diimide compounds in similar solvents.[32] In contrast to strong aggregation of **1b** and **2a**, compounds **1c** and **2b** have a lower K_E value of 18 ± 2 and 326 ± 33 M^{-1}, respectively, indicating that the aggregation of the compounds is greatly suppressed by bulky *t*-butyl groups.

The aggregation of PAMs in solution is also supported by the changes of the absorption extinction coefficient at different concentrations. With compounds **1c**, **2b**, and **3b** as examples (Figure 7), upon increasing the concentration from 2.0×10^{-7} to 2.0×10^{-5} mol/L, the extinction coefficient (0−0 transition) of **1c**, **2b**, and **3b** decreases by 13% (98 000 to 85 000 $M^{-1}cm^{-1}$), 25% (187 000 to 141 000 $M^{-1}cm^{-1}$), and 50% (84 000 to 42 000 $M^{-1}cm^{-1}$), respectively. Furthermore, a noticeable red-shift of absorption for **3b** was also observed upon increasing the concentration gradually. Therefore, the tendency in molecular aggregation is clearly correlated with the molecular length for PAMs, as supported by the aforementioned concentration- and temperature-dependent ^1H NMR studies.

The electrochemical properties of all the PAMs in dichloromethane, except for **4a** because of its poor solubility, were studied in a three-electrode electrochemical cell with Bu_4NClO_4 (0.1 M) and Ag/AgCl as electrolyte and reference electrode, respectively, and the data are collected in Table 1. These compounds exhibit a reversible or quasi-reversible redox process in the negative potential region, indicative of the *n*-type doping nature. It was found that *t*-butyl groups had almost no effect on the redox properties of PAMs. Depicted in Figure 8 are the cyclic voltammograms of compounds **1c**, **2**−**4b**, and **5**. Compound **1c** exhibits one reversible reduction wave at −1.22 V vs Ag/AgCl together with the second quasi-reversible reduction wave at −1.40 V. Compounds **2b** and **3b** also exhibit two reduction waves. The first reduction wave of compounds **2b** and **3b** is shifted by 440 mV to more positive potential compared to that of compound **1c**, suggesting the enhanced electron affinity is due to introduction of two more pyrazine units. With addition of another two fused pyrazine units, compounds **4b** and **5** show three reduction waves along with the more positive first reduction waves. Compared to that of compounds **2b** and **3b**, the first reduction wave of compounds **4b** and **5** is shifted by about 70 mV to −0.73 and −0.71 V, respectively, which are very close to that of [6,6]-phenyl-C_{61}-butyric acid methyl ester (PCBM),[10d] a state-of-the-art *n*-type semiconductor. This implies that PAMs are potential *n*-type semiconductors. It is interesting to note that PAMs with the same number of pyrazine units have the identical first reduction potential (Table 1), suggesting that the electron affinity of these PAMs largely depends on the number of pyrazine units.[33]

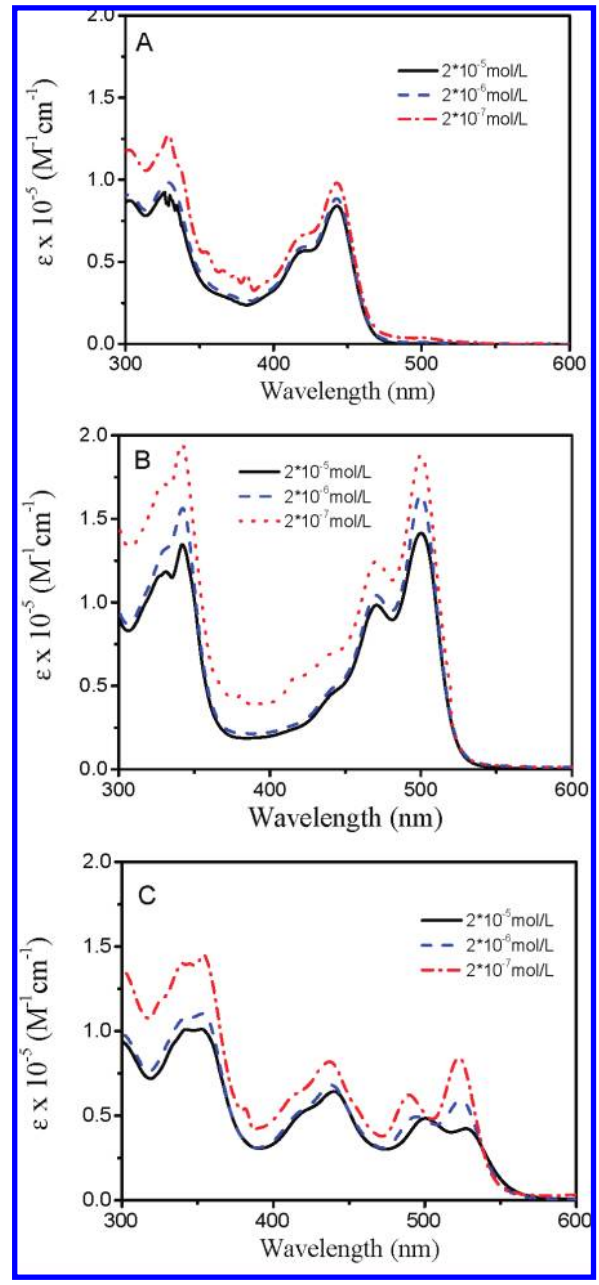

Figure 7. Concentration-dependent UV−vis spectra of **1c** (A), **2b** (B), and **3b** (C) in *d*-chloroform at 20 °C.

The lowest unoccupied molecular orbital (LUMO) energy levels of **1**−**5** were estimated from the reduction onset potentials calibrated by the ferrocene/ferrocenium pair.[34] As shown in Table 1, with an increase in molecular length, the LUMO energy levels decreased from −3.24 eV for **1c** to −3.78 eV for **5**. Meanwhile, introduction of alkoxyphenyl terminal groups and

(31) (a) Hoger, S.; Bonrad, K.; Mourran, A.; Beginn, U.; Moller, M. *J. Am. Chem. Soc.* **2001**, *123*, 5651–5659. (b) Tobe, Y.; Utsumi, N.; Kawabata, K.; Nagano, A.; Adachi, K.; Araki, S.; Sonoda, M.; Hirose, K.; Naemura, K. *J. Am. Chem. Soc.* **2002**, *124*, 5350–5364. (c) Nakamura, K.; Okubo, H.; Yamaguchi, M. *Org. Lett.* **2001**, *3*, 1097–1099.

(32) (a) Wang, W.; Li, L.-S.; Helms, G.; Zhou, H.-H.; Li, A. D. Q. *J. Am. Chem. Soc.* **2003**, *125*, 1120–1121. (b) Wang, W.; Han, J. J.; Wang, L.-Q.; Li, L.-S.; Shaw, W. J.; Li, A. D. Q. *Nano Lett.* **2003**, *3*, 455–458. (c) Li, A. D. Q.; Wang, W.; Wang, L.-Q. *Chem.−Eur. J.* **2003**, *9*, 4594–4601.

(33) (a) Lee, S. K.; Zu, Y.; Herrmann, A.; Geerts, Y.; Müllen, K.; Bard, A. J. *J. Am. Chem. Soc.* **1999**, *121*, 3513–3520. (b) Fogel, Y.; Kastler, M.; Wang, Z.; Andrienko, D.; Bodwell, G. J.; Müllen, K. *J. Am. Chem. Soc.* **2007**, *129*, 11743–11749.

(34) (a) Parker, V. D. *J. Am. Chem. Soc.* **1976**, *98*, 98–103. (b) Eckhardt, H.; Shacklette, L. W.; Jen, K. Y.; Elsenbaumer, R. L. *J. Chem. Phys.* **1989**, *91*, 1303–1315.

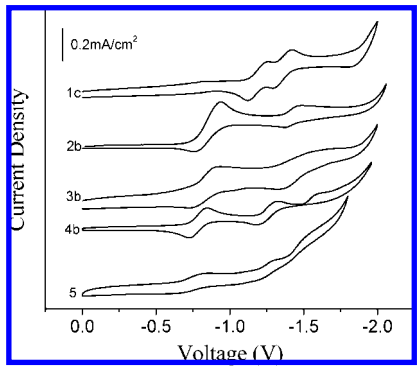

Figure 8. Cyclic voltammograms of **1c**, **2b**, **3b**, **4b**, and **5** in dichloromethane at a scan rate of 0.1 V/s.

t-butyl substituents showed no effect on the LUMO energy levels of PAMs.

Conclusions

Under the optimized condensation conditions, 10 acene-type compounds (**1**−**5**) containing 2−6 pyrazine units and up to 16 rectilinearly arranged fused aromatic rings were synthesized. To the best of our knowledge, compound **5**, with 16 rectilinearly arranged fused aromatic rings and a length about 5 nm, is the longest acene-type conjugated molecule. Absorption measurements reveal that the energy gap of the molecules decreases with an increase in the molecular length. All these molecules tend to aggregate in solution, which can be greatly suppressed by introducing bulky *t*-butyl groups. The *n*-type semiconductor nature of these acene-type compounds has been verified by the electrochemical data. With the increasing number of pyrazine rings and the increasing length of the molecules, the electron affinity of these compounds is significantly enhanced. As a result, the LUMO energy levels decrease from −3.24 to −3.78 eV, comparable to a well-known *n*-type PCBM material. High electron affinity, high environmental stability, and ease of structural modification make these compounds excellent candidates as a new class of *n*-type semiconductors.

Acknowledgment. This work was supported by the National Natural Science Foundation of China (Nos. 20574067 and 50633040), Science Fund for Creative Research Groups (No. 20621401), and 973 project (2002CB613402). We also thank Professor Zhi Yuan Wang at Carleton University of Canada for his help with manuscript revision.

Supporting Information Available: All experimental details, including synthesis and characterization of all compounds and thermogravimetric analysis results (PDF, CIF). This material is available free of charge via the Internet at http://pubs.acs.org.

JA800311A